Available online at www.sciencedirect.com

SciVerse ScienceDirect

Procedia Engineering 57 (2013) 1319 – 1328

Procedia Engineering

www.elsevier.com/locate/procedia

11th International Conference on Modern Building Materials, Structures and Techniques, MBMST 2013

# Assessment of Concrete Bridge Performance under Moderate Seismic Shock Using Concrete Damage Plasticity Model

Joanna M. Dulinska[a,*], Radoslaw Szczerba[b]

[a]Faculty of Civil Engineering, Cracow University of Technology, Warszawska 24, 31-155 Krakow, Poland
[b]Faculty of Civil Engineering, Rzeszow University of Technology, Powstancow Warszawy 12, 35-959 Rzeszow, Poland

**Abstract**

In the paper the assessment of seismic performance of the reinforced concrete bridge to the moderate earthquake is presented. To represent the inelastic behaviour of the concrete material under dynamic loading the concrete damage plasticity model was assumed. The seismic input data were registered during the most recent natural seismic shock that occurred in Poland on 6th January 2012. A model of non-uniform kinematic excitation, typical for multiple-support structures, was introduced. The analysis proved that the first natural frequency of the bridge lied in the range of dominant frequencies of the shock that caused the amplification of the dynamic response. It turned out that the tensile damage (cracking) in some parts of the bridge appeared and the stiffness of the concrete material was degraded even under moderate seismic event. Hence, the seismic resilience of the bridge decreased after the shock. This is especially important not only in case of earthquake but in case of mining tremors as well. Considering their high repeatability the concrete material might be gradually degraded.



*Keywords*: concrete bridges; bridge dynamics; non-linear dynamic analysis; dynamic response; concrete damage plasticity model; seismic analysis.

## 1. Introduction

A wide range of structural analysis methods is applied nowadays for bridges located in earthquake zones. The level of sophistication of these methods depends on the purpose of the analysis. Bridges located in areas of high seismicity can receive severe damage and failures during strong seismic phenomena. Hence, the assessment of their dynamic performance is usually conducted on the basis of nonlinear time history analysis [1-4] or nonlinear pushover analysis [5]. In case of the assessment of seismic behaviour of bridges located in moderate seismicity zones or in mining tremor areas authors often use simpler linear methods [6-7].

However, for concrete bridges with relatively short piers, the first natural frequency of vibration may be located in a range of dominant frequencies of earthquake ground motions, particularly when founded on rock or hard soil. Then, the seismic response of the structure even to a moderate shock might be amplified by the resonance effect. This is also especially important in case of mining tremors of high repeatability, which often occur in mining activity areas and which resemble moderate natural shocks. Hence, an appropriate and realistic representation of the concrete material is essential for the assessment of the performance of bridges under moderate seismic events to reflect possible nonlinear performance of the structure. The nonlinear response of the bridge may be caused by cracking of concrete in tension. The cracking process has a great influence on the mechanical behavior of concrete, since propagation of cracks during loading contributes to the nonlinear behavior at low stress levels.

* Corresponding author.
*E-mail address:* jdulinsk@pk.edu.pl


doi:10.1016/j.proeng.2013.04.166

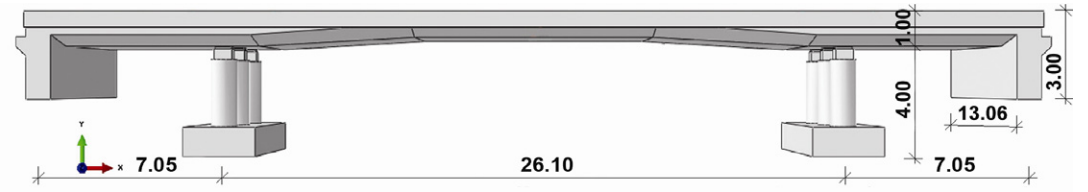


Fig. 1. Scheme and main dimensions of the bridge

This paper presents an advanced nonlinear time history analysis of a concrete bridge subjected to a real seismic event registered recently in the territory of Poland. The constitutive model of concrete damage plasticity, provided by ABAQUS software [8], was incorporated in the calculations. It assumes two mechanisms of failure of the concrete material: tensile cracking and compressive crushing [9-10]. The material is damaged or degraded due to the elastic stiffness degradation characterized by the scalar variables for tension and compression.

## 2. The main data of the investigated bridge structure

In the calculations of the dynamic response to a moderate seismic event a reinforced concrete bridge with steel-laminated elastomeric bearings was considered. A finite element model of the structure was based on a geometry of an existing three-span bridge located in Poland [11].

Fig. 1 shows the main dimensions of the bridge. The length of the central span was 26.1 m. The three piers of 2.95 m high with a diameter of 1.1 m were located regularly at a distance of 3.75 m. The abutments were situated 7.05 m away from the extreme piers. The fixed boundary conditions reflected the high rigidity of the foundation rock.

The bridge was equipped with elastomeric bearings as linking elements between the deck of the bridge and piers. The cross sectional area of the bearing was determined by the allowable pressure on the bearing support. The length and the width were both assumed 0.6 m. The bearing was composed of two steel cover plates, each 20 mm thick, between which elastomeric laminae reinforced with steel shims were placed. The thickness of one elastomeric layer was assumed 8 mm, the thickness of one steel reinforcement layer was 3 mm. Fig. 2 presents the steel-laminated elastomeric bearing.

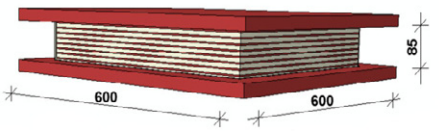


Fig. 2. The steel-laminated elastomeric bearing

For elastomeric bearings a two-coefficient Mooney-Rivlin model is usually used as a constitutive model for hyperelastic nonlinear elastomeric materials. However, the parameters of the Mooney-Rivlin model: $C_{10}$ and $C_{01}$ can be replaced with equivalent elasticity modulus [12]: $E = 6\,(C_{10} + C_{01})$. Hence, in this paper the parameters of the Mooney-Rivlin model assumed for the calculations, $C_{10} = 0.292$ MPa and $C_{01} = 0.177$ MPa, were replaced with the equivalent elasticity modulus 2.814 MPa. The Poisson's ratio of the elastomeric bearing was taken as 0.49. For the steel shims the elasticity modulus 210 GPa and Poisson's ratio 0.3 were considered.

In summary, the 3D numerical model of the bridge, shown in Fig. 3, was discretized by 58843 tetrahedral 10-node finite elements [8].

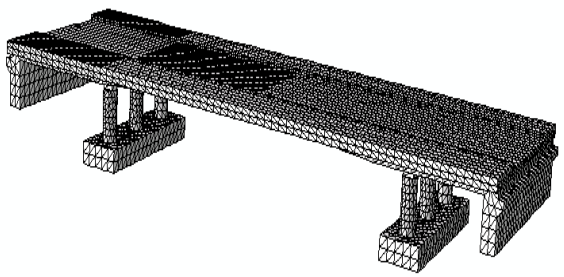

Fig. 3. Three dimensional numerical model of the bridge discretized by 58843 tetrahedral 10-node finite elements

As a first step, preceding the seismic analysis, the natural frequencies of the bridge were evaluated. The lowest natural frequency was $f_1 = 3.9$ Hz. Then, the coefficient of the Rayleigh model of damping was calculated. The stiffness proportional damping was applied with a coefficient $\beta = 2\xi_1/\omega_1$. This coefficient was determined for damping ratio $\xi_1 = 5$ % referring to the first circular frequency $\omega_1 = 2\,\pi\, f_1$.

## 3. Constitutive parameters for concrete damage plasticity model used for bridge calculations

To represent the elastic-plastic behavior of the bridge under a seismic shock the concrete damage plasticity model was assumed as a constitutive model for the concrete material [9-10], [13]. The model [8] consists of the combination of non-associated multi-hardening plasticity and scalar damaged elasticity to describe the irreversible damage that occurs during the fracturing process. The yield surface is controlled by two variables representing equivalent plastic strains: $\tilde{\varepsilon}_t^{pl}$ and $\tilde{\varepsilon}_c^{pl}$, associated with failure mechanisms under tension and compression loading, respectively. The degradation of the elastic stiffness is characterized by two different damage variables: $d_t$ – for tension and $d_c$ – for compression. These variables are functions of equivalent plastic strains. They can take values from zero – which represents undamaged material, to one – which denotes total loss of strength. The concrete damage plasticity model is specially recommended for calculations of concrete structures subjected to dynamic loadings, like earthquakes [8], [9-10], [14].

The essential constitutive parameters of the model are summarized in Table 1 [15]. These properties were obtained through laboratory tests.

Table 1. Constitutive parameters of the concrete damage plasticity model [15]

| Concrete tension stiffening | | Concrete tension damage | |
|---|---|---|---|
| Stress [MPa] | Cracking strain [-] | $d_t$ [-] | Cracking strain [-] |
| 1.99893 | 0.0 | 0.0 | 0.0 |
| 2.842 | 0.00003333 | 0.0 | 0.00003333 |
| 1.86981 | 0.000160427 | 0.406411 | 0.000160427 |
| 0.862723 | 0.000279763 | 0.69638 | 0.000279763 |
| 0.226254 | 0.000684593 | 0.920389 | 0.000684593 |
| 0.056576 | 0.00108673 | 0.980093 | 0.00108673 |
| Concrete compression hardening | | Concrete compression damage | |
| Stress [MPa] | Crushing strain [-] | $d_c$ [-] | Crushing strain [-] |
| 15.0 | 0.0 | 0.0 | 0.0 |
| 20.197804 | 0.0000747307 | 0.0 | 0.0000747307 |
| 30.000609 | 0.0000988479 | 0.0 | 0.0000988479 |
| 40.303781 | 0.000154123 | 0.0 | 0.000154123 |
| 50.007692 | 0.000761538 | 0.0 | 0.000761538 |
| 40.236090 | 0.002557559 | 0.195402 | 0.002557559 |
| 20.236090 | 0.005675431 | 0.596382 | 0.005675431 |
| 5.257557 | 0.011733119 | 0.894865 | 0.011733119 |

Other parameters of the concrete material were taken as follows: elasticity modulus 19.7 GPa, Poisson's ratio 0.19 and dilation angle 38°. The mass density of the concrete was chosen as 2400 kg/m$^3$.

## 4. Seismic input data

Although Poland is located in a low seismicity zone and the return periods of earthquakes are relatively long, the seismic hazard of Poland is continuously monitored by seismological stations run by the Institute of Geophysics Polish Academy of Science [16]. Some historical seismic events proved that even in very low seismicity zones natural phenomena, strong enough to damage structures located close to the epicentres of the shocks, may happen.

According to the historical seismic events and current registrations of earthquakes maps of seismic hazard were established for Poland and neighbouring countries. The evaluation of seismic risk for particular zone involves defining maximal horizontal acceleration which can appear in that zone with certain return period. Figure 4 presents an earthquake

hazard map for Poland, Czech and Slovakia [17]. The map shows seismic risk in peak ground acceleration (PGA) with the return period of 1000 years.

It could be noticed from the presented map of the seismic hazard that the vast majority of Poland is a located in a very low seismicity zone. But it also could be observed from Fig. 4, that the region along the southern frontier of Poland (the width of 100 km) could be exposed to larger values of peak ground accelerations (i.e. Kotlina Kłodzka, Beskid Żywiecki, Podhale, Beskid Sadecki). The maximal PGA reaches even 1,6 m/s$^2$.

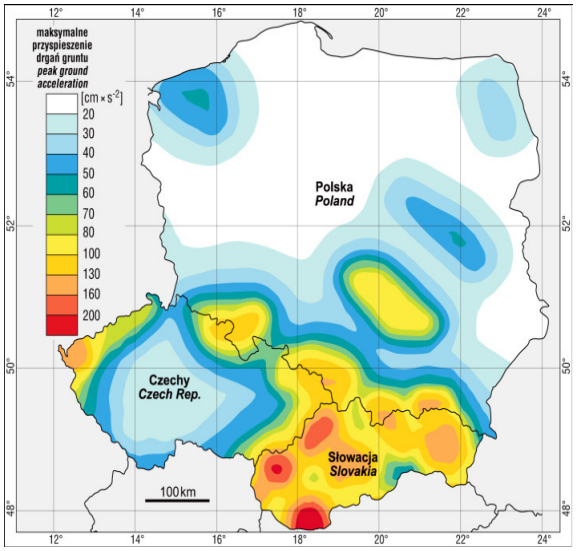


Fig. 4. Earthquake hazard map in peak ground acceleration with the 90% probability of non-exceedance within 105 years (the return period of 1000 years) (Schenk *et al.* 2001)

The time histories of acceleration in three directions (horizontal direction WE, horizontal direction NS, vertical Z) applied for dynamic analysis as kinematic excitations of the bridge are shown in Fig. 5. These data are based on the registration of the most recent natural seismic shock that occurred in Poland on 6th January 2012. It was one the strongest shocks ever recorded in Polish territory. The epicenter of this phenomenon was located near Jarocin, Poland. The magnitude of the shock was 3.8 in Richter scale. The peak ground accelerations in WE direction reached a value of 0.0015 m/s$^2$, 0.001 m/s$^2$ in NS direction and 0.0006 m/s$^2$ in vertical direction.

For the purpose of this study the registered data were scaled up, so the peak ground acceleration raised to 0.4 m/s$^2$ in WE direction, 0.3 m/s$^2$ in NS direction and 0.015 m/s$^2$ in vertical direction Z. It means that the investigated bridge is situated in the zone with maximal horizontal peak ground acceleration of the shock equal 0.5 m/s$^2$. The scaled records were also filtered to a maximum frequency of 10 Hz.

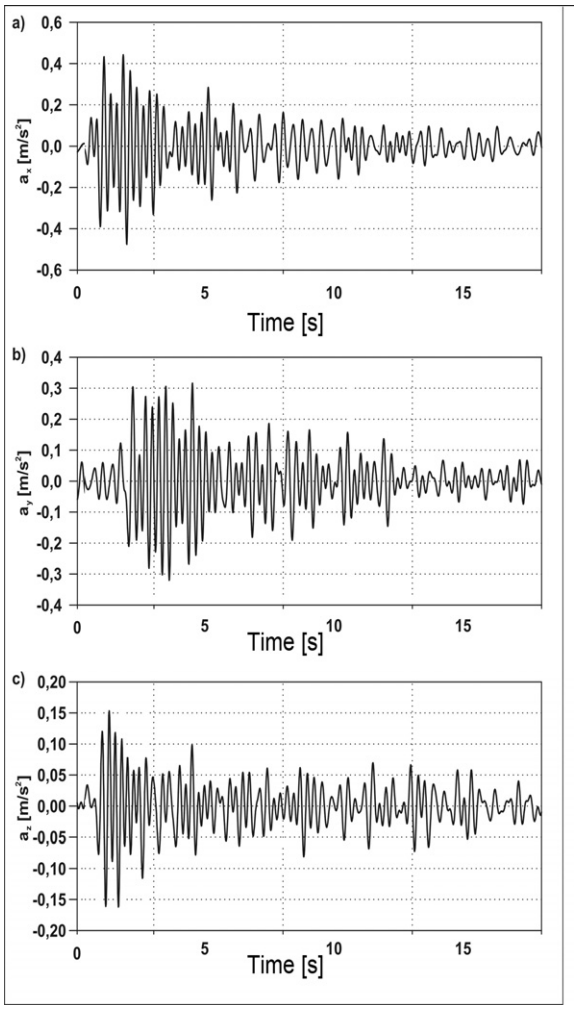


Fig. 5. Time histories of ground accelerations: (a) horizontal direction WE; (b) horizontal direction NS; (c) vertical direction Z

Fig. 6 presents the power spectral density (PSD) function of accelerations in WE direction (see Fig. 5a) obtained from signal processing. It could be concluded on the basis of Fig. 6 that the dominant frequencies of the earthquake ground motions in WE direction are located in the range from 3.5 to 4.2 Hz. Similar dominant range of frequencies were also obtained for NS and Z directions.

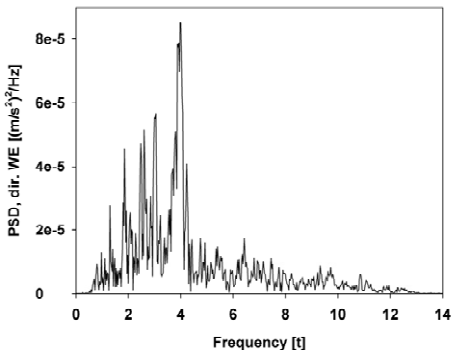


Fig. 6. Frequency spectrum (PSD function) of accelerations registered in WE direction

The comparison of the frequency spectrum of the shock with the first natural frequency of the bridge (3.9 Hz) indicates that the resonance effect leading to the amplification of ground vibrations may occur. This effect is pointed out by authors who investigate bridges with short piers [18].

## 5. Analysis of the dynamic response of the bridge to the moderate seismic shock

The dynamic response of the bridge to the moderate seismic shock was calculated by time history analysis. The Hilber-Hughes-Taylor direct-integration method was used for the solution of the equation of motion [8]. A small step increment of 0.001 s was introduced for this highly nonlinear analysis to obtain convergence.

In calculations non-uniform kinematic excitation was taken into consideration [19-20], [7]. It was assumed that the seismic wave propagated along the bridge and that the subsequent supports repeated the same motion with a time delay dependent on the wave velocity. The wave velocity was 300 m/s.

The evolution of tensile damage in the middle bottom part of the bridge deck during the entire shock is illustrated in Fig. 7. Firstly, the static analysis of dead load indicates that the concrete material of the bridge generally remained with no tensile damage and no stiffness degradation. The exception is Point A located in the middle bottom part of the bridge deck, see Fig. 7a.

Secondly, it could be observed that during the intensive part of the shock considerable plastic strains were developing. The middle bottom part of the bridge deck was affected by progressive tensile damage and elastic stiffness degradation. In Figs 7b and 7c, which correlate to the condition of the deck in $t_2 = 2.18$ s and $t_3 = 2.29$ s, the increase in tensile damage at several points could easily be noticed (i.a. Point B).

Finally, the situation at the end of the intensive phase of the shock ($t_4 = 15$ s) is presented in Fig. 7d. The points at which the concrete material was degraded are clearly demonstrated. The scale of the variable $d_t$ depicts the level of total tensile damage at points of the bridge deck.

The evolution of tensile damage and elastic stiffness degradation of the middle bottom part of the bridge deck could also be clearly observed in Fig. 8 and Fig. 9, which refer to Points A and B, respectively. Point A is the most exposed to tension point of the deck. At Point A the process of cracking initiated under the dead load because at the end of the static stage the tensile equivalent plastic strains were already greater than zero. Than the large increment in equivalent plastic strains occurred at time $t_2 = 2.18$ s. This moment correlates with the significant increase in both horizontal accelerations of the ground motion, see Fig. 5a, b. The further increase in equivalent plastic strains at Point A is not very significant.

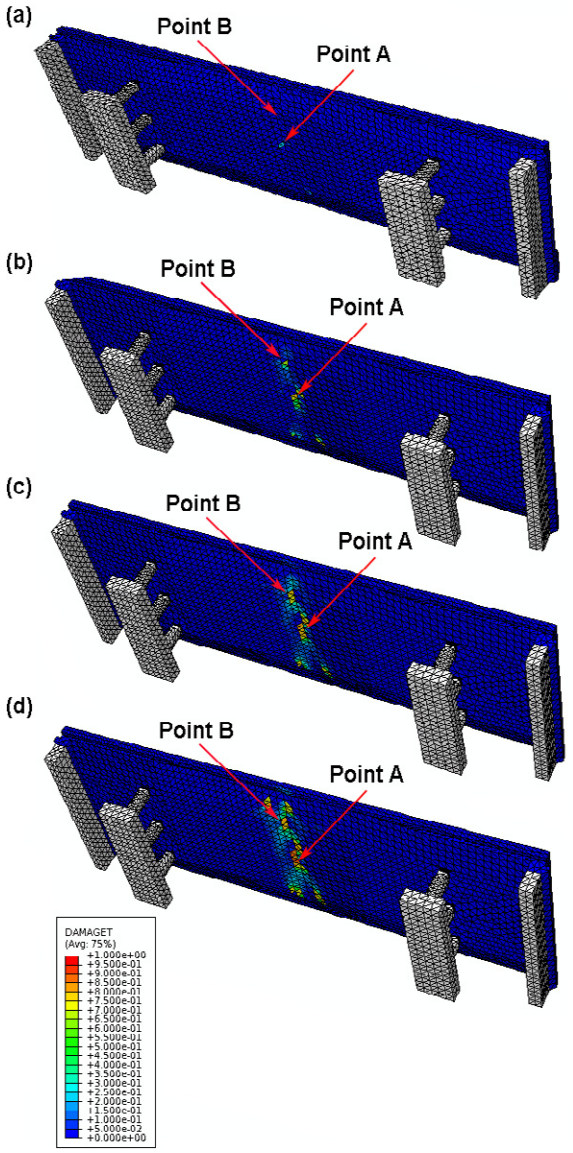


Fig. 7. Evolution of tensile damage of the middle bottom part of the bridge deck: (a) $t_1$= 0.0 s (dead load only); (b) $t_2$=2.18 s (shock in progress); (c) $t_3$=2.29 s (shock in progress); (d) $t_4$=15 s (end of the intensive phase of the shock)

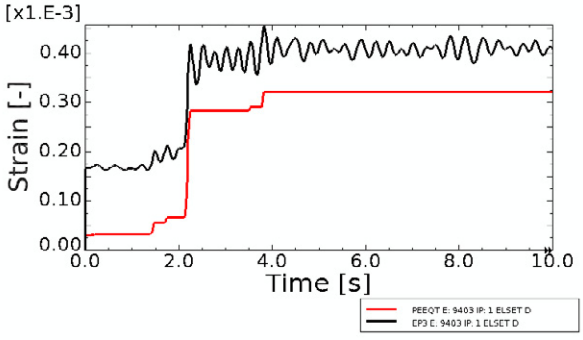


Fig. 8. Time history of maximal principal strains (black line) and equivalent plastic strains (red line) at Point A

In Fig. 9 the time history of strains at Point B, which is less exposed to tension than Point A, is shown. In that point the equivalent plastic strain was zero at the end of the static stage, but further time history of equivalent plastic strains also reflects the time history of kinematic excitation. The final level of the equivalent plastic strains at Point B is three times lower than at Point A.

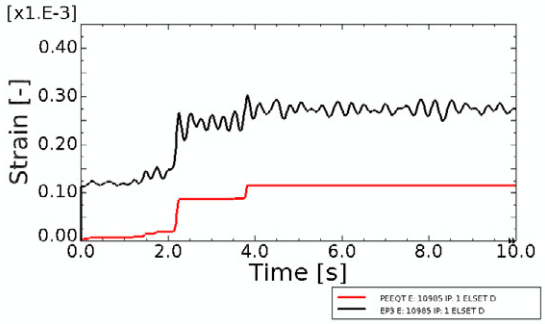


Fig. 9. Time history of maximal principal strains (black line) and equivalent plastic strains (red line) at Point B

Not only the middle bottom part of the bridge deck was affected with the elastic stiffness degradation due to tensile process during the shock. The concrete material is degraded also at a few points of the upper part of the deck above both piers. In Fig. 10 the distribution as well as the level of the damage variable $d_t$ on the upper surface of the bridge deck are demonstrated. The dead load result in a very small tensile damage (cracking) area on the upper surface of the deck, see Fig. 10a. At the end of the seismic event the number of elements on the upper surface of the deck above the piers with degraded stiffness slightly increases.

In Fig. 11 the time history representing the accumulation of equivalent plastic strains during the shock at Point C is shown. The character of curves in Fig. 11 resembles the time histories of strains at Points A and B, but the level of equivalent plastic strains is definitely lower.

Finally, the time histories of vertical displacements at Point A located at the middle bottom part of the deck as well as at Point C situated at the upper surface of the deck above the pier are presented in Fig. 12.

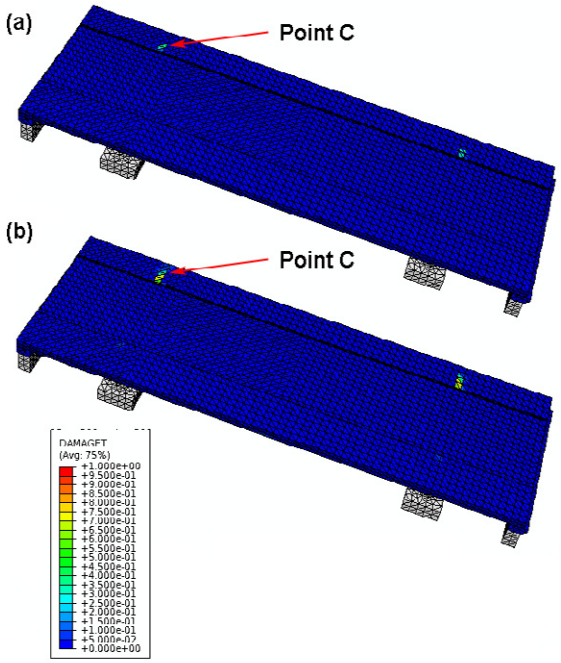


Fig. 10. Evolution of tensile damage of the upper part of the deck: (a) $t_1$= 0.0 s (dead load only); (b) $t_4$=15 s (end of the intensive phase of the shock)

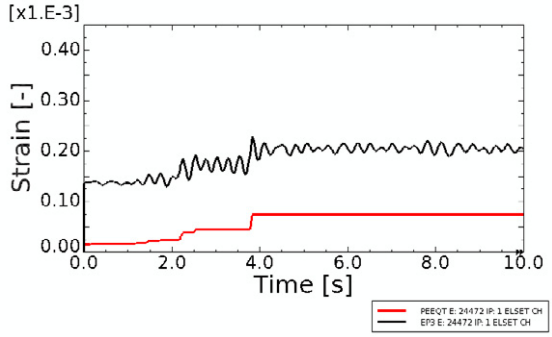


Fig. 11. Time history of maximal principal strains (black line) and equivalent plastic strains (red line) at Point C

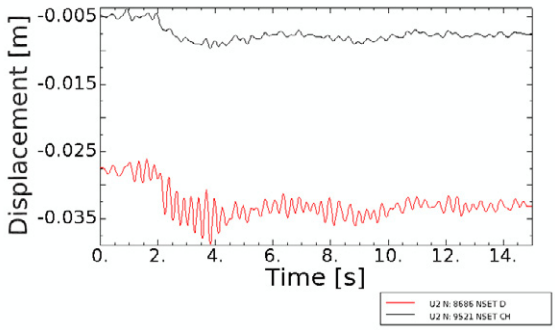


Fig. 12. Time history of displacements at Point A on the middle bottom part of the deck (red line) and at Point C on the upper surface of the deck above the pier (black line)

It could be noticed from Fig. 12 that the static displacement at Point A located in the middle of the bridge was about 2.75 cm. Then, additional displacements temporarily appeared during the shock and reached a value of 3.8 cm in total. After the shock the vertical displacement increased to 3.25 cm, that is due to the plastic behaviour of the concrete material. Similar situation occurred at Point C on the upper surface of the deck, however the displacements were much smaller than in the middle of the deck.

## 6. Conclusions

In the paper the results of calculations of the dynamic responses of the concrete bridge to the moderate seismic shock were presented and assessed. To represent inelastic behaviour of the bridge the concrete damage plasticity model was assumed. The model allowed to describe the irreversible tensile damage that occurred during the dynamic loading. In summary, the following conclusions as well as some general remarks for engineering practice can be formulated:

- The appropriate and realistic representation of the concrete material is essential for the assessment of dynamic performance of bridges located in moderate seismicity zones.
- It is proved by the results of the nonlinear dynamic analysis that even moderate seismic phenomenon could result in tensile damage and stiffness degradation of the concrete bridge deck, especially if the natural frequencies of the bridge fall into the range of the dominant frequencies of the shock.
- The seismic resilience of the bridge decreased after the moderate seismic shock as a result of tensile damage and stiffness degradation.

This conclusion may be of a special importance also in case of mining tremors which occur in mining activity areas and which resemble the mechanism of moderate earthquakes. Considering the high repeatability of mining tremors the concrete material may be gradually degraded during the time of exploitation of the bridge.

## References

[1] Phung, V., Lau, D., 2008. "Three-dimensional nonlinear degrading model for earthquake response analyses of concrete bridges", Proc. of the 14th World Conference on Earthquake Engineering, October 12-17, 2008, Beijing, China.
[2] Sextos, A.G., Pitilakis, K.D., Kappos, A. J., 2003. Inelastic dynamic analysis of RC bridges accounting for spatial variability of ground motion, site effects and soil–structure interaction phenomena. Part 1: Methodology and analytical tools, Earthquake Engineering Structural Dynamics 32(4), pp. 607–627.
[3] Sextos, A. G., Pitilakis, K. D., Kappos, A. J., 2003. Inelastic dynamic analysis of RC bridges accounting for spatial variability of ground motion, site effects and soil-structure interaction phenomena. Part 2: Parametric Study, Earthquake Engineering and Structural Dynamics 32(4), pp. 629-652.
[4] Sextos, A. G., Kappos, A. J., 2009. Evaluation of seismic response of bridges under asynchronous excitation and comparisons with Eurocode 8-2 provisions, Bulletin of Earthquake Engineering 7(2), pp. 519–545.
[5] Paraskeva, Th., Kappos, A. J., Sextos, A.G., 2006. Extension of modal pushover analysis to seismic assessment of bridges, Earthquake Engineering and Structural Dynamics 35(1), pp. 1269-1293.
[6] Bardakis, V. G., Fardis, M.N., 2011. Nonlinear dynamic v. elastic analysis for seismic deformation demands in concrete bridges having deck integral with the piers, Bulletin of Earthquake Engineering 9(2), pp. 519-535.
[7] Dulinska, J. M., 2011. Influence of wave velocity in the ground on dynamic response of large dimensional structures, International Journal of Earth Sciences and Engineering 5(4), pp. 538-541.
[8] ABAQUS, Users Manual V. 6.10-1. 2010. Dassault Systemes Simulia Corp., Providence, RI.
[9] Lee, J., Fenves, G. L., 1998. Plastic-Damage Model for Cyclic Loading of Concrete Structures, Journal of Engineering Mechanics 124(8), pp. 892–900. doi:10.1061/(ASCE)0733-9399(1998)124:8(892)
[10] Lee, J., Fenves, G. L., 1998. A Plastic-Damage Concrete Model for Earthquake Analysis of Dams, Earthquake Engineering and Structural Dynamics 27(9), pp. 937–956.
[11] Dulinska, J. M., Szczerba, R., 2013. Simulation of dynamic behaviour of reinforced concrete bridge with steel-laminated elastomeric bearings under high-energy mining tremors, Key Engineering Materials 531–532: pp. 662-668. doi:10.4028/www.scientific.net/KEM.531-532.662.
[12] Buckle, I.; Nagarajaiah, S.; Ferrell, K. ,2002. Stability of Elastomeric Isolation Bearings: Experimental Study, *Journal of Structural Engineering* 128 (1): 3-11.
[13] Lubliner, J., Oliver, S., Oller, E., Onate, A., 1989. Plastic-Damage Model for Concrete, International Journal of Solids and Structures 25(3), pp. 229-326.
[14] Dulinska, J. M., 2013. Cooling tower shell under asynchronous kinematic excitation using concrete damaged plasticity model, Key Engineering Materials 535-536: pp. 469-472, doi:10.4028/www.scientific.net/KEM.535-536.469.
[15] Jankowiak, T.; Lodygowski, T. 2005. Identification of parameters of concrete damage plasticity constitutive model, Foundations of Civil and Environmental Engineering 6, pp. 53-69.
[16] Geophysical monitoring [online]. Institute of Geophysics, Polish Academy of Sciences [cited 10 February 2013]. Available from Internet: www.igf.edu.pl/en/monitoring _geofizyczny
[17] Schenk, V., Schenkova, Z., Kottnauer, P., Guterch, B., Labak, P., 2001. Earthquake hazards maps for the Czech Republic, Poland and Slovakia, Acta Geophysica Polonica 49(3), pp. 287–302.
[18] Abdel Raheem, S. E., Hayashikawa, T., 2008. "Innovative control strategy for seismic pounding mitigation of bridge structures", Proc. of the 14th World Conference on Earthquake Engineering, October 12-17, 2008, Beijing, China.
[19] EN 1998-2:2005 Eurocode 8 - Design of structures for earthquake resistance. Part 2: Bridges, ENV 1998-2, CEN, Brussels.
[20] Zerva, A., 2009. Spatial variation of seismic ground motion. Modeling and engineering applications. CRC Press, Taylor & Francis Group, Boca Raton, FL, p. 460.